

D. KUC\*, E. HADASIK\*, I. SCHINDLER\*\*, P. KAWULOK\*\*, R. ŚLIWA\*\*\*

## CHARACTERISTICS OF PLASTICITY AND MICROSTRUCTURE OF HOT FORMING MAGNESIUM ALLOYS Mg-Al-Zn TYPE

### CHARAKTERYSTYKI PLASTYCZNOŚCI I MIKROSTRUKTURA ODKSZTAŁCANYCH NA GORĄCO STOPÓW MAGNEZU TYPU Mg-Al-Zn

The paper presents analysis of plasticity characteristics and microstructure of magnesium alloys for hot plastic treatment with different aluminium content (3÷8%). Tests were conducted for assessment of susceptibility of tested alloys to hot plastic deformation. A tensile test was run in temperature from 250 to 450°C. Based on the results, ultimate tensile strength (UTS) and reduction of area (Z) were determined for samples. Conducted compression tests allowed to specify the flow stress and microstructure changes after deformation. The activation energy in hot forming was determined for investigated alloys. The parameters of the process where flow is significantly influenced by twin formation in microstructure were determined. A varied plasticity of tested alloys was found depending on aluminium content. Test results will be useful in development of forging technology of selected construction elements which serve as light substitutes for currently used materials.

*Keywords:* magnesium alloy, research of plasticity, microstructure, dynamic recrystallization, activation energy

W pracy analizowano charakterystyki plastyczności i mikrostrukturę stopów magnezu przeznaczonych do przeróbki plastycznej na gorąco ze zróżnicowaną zawartością aluminium (3÷8%). Badania prowadzono dla oceny podatności badanych stopów do kształtowania plastycznego w warunkach przeróbki plastycznej na gorąco. Przeprowadzono próbę rozciągania w temperaturze od 250 do 450°C, na podstawie której określono wytrzymałość na rozciąganie i przewężenie badanych próbek. Wykonane próby ściskania pozwoliły na wyznaczenie naprężenia uplastyczniającego i zmian mikrostruktury po odkształceniu. Dla badanych stopów wyznaczono energię aktywacji odkształcenia plastycznego na gorąco. Określono parametry procesu, dla których na przebieg plastycznego płynięcia wpływa istotnie bliźniakowanie w mikrostrukturze. Wykazano zróżnicowaną plastyczność badanych stopów w zależności od zawartości aluminium. Wyniki badań będą pomocne do opracowania technologii kucia wybranych elementów konstrukcyjnych stanowiących lekkie zamienniki stosowanych obecnie materiałów.

#### 1. Introduction

Since the beginning of the 21<sup>st</sup> century, one can observe significant increase of the interest in magnesium alloys as applied in automotive and aerospace industry, as well as in space technology [1, 2]. The development of deformable magnesium alloys and plastic forming methods has been strongly limited so far [3, 4]. A very popular group of magnesium alloys are those containing aluminium with addition of zinc and manganese. Such materials, due to the used ingredients, are relatively cheap. They are characterised by beneficial set of mechanical properties. The most popular is alloy AZ31 which is characterised by good deformability and is processed in conditions of rolling, extrusion or forging. Resistance of the alloys from this group increases with the increase of aluminium content. For elements which are supposed to have bigger resistance it is better to use alloys marked as AZ61 and AZ80 which include 6 and 8% aluminium respectively. Alloy AZ31 may reach ultimate tensile strength of 260 MPa, alloys AZ61

and AZ80 respectively 325 and 350 MPa after extrusion. Together with increase of aluminium content the plasticity and susceptibility to plastic treatment in lower temperatures decreases [5]. That is why such materials are often used as foundry materials. In order to prepare technology of plastic processing it is necessary to define precisely the plastic properties and microstructure changes of those alloys. The aim of the paper was to compare the plasticity and microstructure of magnesium alloys with from 3 to 8% aluminium content from group Mg-Al-Zn-Mn. On the basis of tensile tests the plasticity changes were determined in temperature from 250 to 450°C. Conducted compression test in temperature from 250 to 450°C and strain rate from 0.01 to 10 s<sup>-1</sup> provided important data concerning the influence of process parameters on flow stress and microstructure changes connected with recrystallization process. The dependencies of flow stress and deformation from Zener-Hollomon parameter were determined. Achieved results will be used for preparation of forging construction elements technology for aviation industry.

\* SILESIA UNIVERSITY OF TECHNOLOGY, FACULTY OF MATERIALS ENGINEERING AND METALLURGY, 40-019 KATOWICE, 8 KRASIŃSKIEGO STR., POLAND

\*\* VSB – TECHNICAL UNIVERSITY OF OSTRAVA, FACULTY OF METALLURGY AND MATERIALS ENGINEERING, 17. LISTOPADU 15, 708 33 OSTRAVA – PORUBA, CZECH REPUBLIC

\*\*\* RZESZOW UNIVERSITY OF TECHNOLOGY, FACULTY OF MECHANICAL ENGINEERING AND AERONAUTICS, 35-959 RZESZÓW, 8 POWSTAŃCÓW WARSZAWY AV., POLAND

## 2. Experimental procedure

The initial materials were rolled bars of magnesium alloy AZ31, AZ60 and AZ80 with diameter of 12 mm and with various aluminium contents. Chemical composition of investigated alloys is presented in Table 1.

Susceptibility of magnesium alloys to cracking in high temperatures was tested on Gleeble 3800 simulator using thread samples with diameter 10 mm and length 125 mm. The tests were conducted at temperatures ranging from 200 to 450°C at deformation rates of 20 mm/s. For samples after tensile test the ultimate tensile strength was determined (UTS) together with area reduction (Z). Cylindrical samples with diameter 10 mm and height 12 mm were used for obtaining the necessary data from the hot deformation simulator Gleeble 3800. They were subjected to uniaxial compression tests.

TABLE 1  
Chemical composition of investigated magnesium alloys, [wt %]

alloys	Al	Zn	Mn	Cu
AZ31	3.0	0.71	0.20	<0.01
AZ61	6.2	0.61	0.22	<0.01
AZ80	8.2	0.34	0.13	<0.03

The tests associated with the study of dynamic softening were conducted at temperatures  $T = 250, 300, 350, 400$  and  $450^\circ\text{C}$  and at the nominal strain rates  $\dot{\varepsilon} = 0.01, 0.1, 1$  or  $10 \text{ s}^{-1}$  (after uniform preheating at temperature of  $450^\circ\text{C}$ ). After attaining the equivalent strain  $\varepsilon = 0.8$  the samples were cooled in water. From values of peak stress  $\sigma_{pp}$  of particular stress-strain curves the value of the activation energy in hot forming was determined and then by means of this value the determination of kinetics of the dynamic recrystallization followed (specifically the strain to reach the peak  $\varepsilon_p$ , corresponding to the dynamic recrystallization start), as a function of Zener-Hollomon parameter (Z).

The apparent activation energy value  $Q$  [ $\text{J} \cdot \text{mol}^{-1}$ ] in hot forming is a key material constant, needed e.g. for calculation of the temperature compensated strain rate represented by the Zener-Hollomon parameter  $Z$  [ $\text{s}^{-1}$ ] [6]:

$$Z = \dot{\varepsilon} \exp\left[\frac{Q}{RT}\right] \quad (1)$$

The knowledge of the given material enables to predict effectively the maximum flow stress value  $\sigma_{pp}$  [MPa] or the strain value  $\varepsilon_p$  [-] corresponding to start of the dynamic recrystallization at the given temperature  $T$  [K] and strain rate  $\dot{\varepsilon}$  [ $\text{s}^{-1}$ ]. The  $Q$ -value should ideally be the material constant depending only on the chemical composition and structure of the given material. The hyperbolic law in Arrhenius type equation is conventionally used for its determination [7]:

$$\dot{\varepsilon} = C \exp\left(\frac{-Q}{RT}\right) \left[\sinh(\alpha\sigma_{pp})\right]^n \quad (2)$$

where  $C$  [ $\text{s}^{-1}$ ],  $n$  [-] and  $\alpha$  [ $\text{MPa}^{-1}$ ] are other material constants,  $R = 8.314 \text{ J} \cdot \text{mol}^{-1} \cdot \text{K}^{-1}$  and  $\sigma_{pp}$  [MPa] is flow stress corresponding to the peak stress on the certain stress-strain curve.

This relationship has been solved by a simple graphic method, based on the repeated application of linear regression. A particularity of the hyperbolic function is used in this calculation that enables to simplify the Eq. (2) for low stress values (i.e. for a high-temperature level) into the form of the Arrhenius power law:

$$\dot{\varepsilon} = C_1 \exp\left[\frac{-Q}{RT}\right] \sigma_{pp}^n \quad (3)$$

and, vice versa, for high stress values (i.e. for a low-temperature level) into the form of the exponential law:

$$\dot{\varepsilon} = C_2 \exp\left[\frac{-Q}{RT}\right] \exp(\beta\sigma_{pp}) \quad (4)$$

where  $C_1$  [ $\text{s}^{-1}$ ],  $C_2$  [ $\text{s}^{-1}$ ] and  $\beta$  [ $\text{MPa}^{-1}$ ] are the material constants. The constant  $\alpha$  in Eq. (2) is given by the relation:

$$\alpha = \frac{\beta}{n} \quad (5)$$

For a chosen high-temperature level the constant  $n$  is determined by the linear regression of the experimental data in coordinates  $\ln \sigma_{pp} \sim \ln \dot{\varepsilon}$ , and for a chosen low-temperature level the constant  $\beta$  is obtained by the linear regression in coordinates  $\sigma_{pp} \sim \ln \dot{\varepsilon}$ . After the calculation of the quantity  $\alpha$  according to the Eq. (5), the constants  $Q$  and  $C$  in Eq. (2) may be calculated by the final linear regression of all the data plotted in the coordinates  $T^{-1} \sim (\ln \dot{\varepsilon} - n \sinh(\alpha\sigma_{pp}))$ .

Such an estimate of constants  $n$  and  $\beta$  can be strongly influenced by the selection of the corresponding temperature level as well as by the experimental data scatter. This weakness has been eliminated by application of the specially developed interactive software ENERGY 4.0 [8]. The program uses the values  $n$  and  $\beta$ , determined by the previous procedure, only as the first estimate of parameters for the final refining multiple nonlinear regression of all the data corresponding to the Eq. (2).

Strain  $\varepsilon_p$  [-] corresponding to the peak stress can be described in dependence on the parameter  $Z$  by the relation [9]:

$$\varepsilon_p = UZ^W \quad (6)$$

where  $U$  [-] and  $W$  [-] are material constants.

The resulting equations describing the dependence peak stress and of the tested materials have the following form:

$$\sigma_{pp} = \frac{1}{\alpha} \arg \sinh\left(\sqrt[n]{\frac{Z}{C}}\right) \quad (7)$$

Equation (7) was obtained by modification of the Eq. (2) after quantification of individual material constants.

Structural examination was performed on a cross-section parallel to the axis of a sample. The samples were included in a conducting material and etched in a solution intended for etching magnesium alloys, containing: 4.2g  $(\text{NO}_2)_3\text{C}_6\text{H}_2\text{OH}$  – picric acid, 70ml  $\text{C}_2\text{H}_5\text{OH}$  – ethyl alcohol, 10ml  $\text{H}_2\text{O}$  – water 10ml  $\text{CH}_3\text{COOH}$  – glacial acetic acid. Structural evaluation was performed using an Olympus GX51 light microscope, in bright field.

### 3. Results

Microstructure of tested alloys in initial condition after extrusion and heating in temperature of 450°C with soaking time of 40 minutes is shown in Fig. 1. Before deformation the tested alloys AZ31 and AZ61 are characterised by single phase microstructure of solution  $\alpha$ -Mg, whereas in microstructure of alloy AZ80 the presence of intermetallic phase  $\gamma$  ( $Mg_{17}Al_{12}$ ) was found and which was confirmed by prior X-ray tests [10, 11].

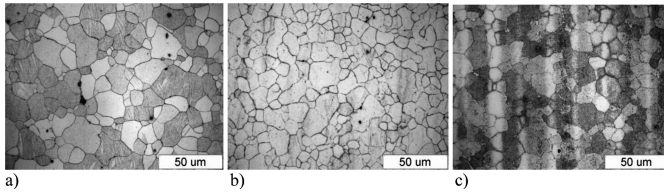


Fig. 1. Microstructure of investigated alloy in initial state after annealing at temperature 450°C with holding time of 40 min. a – AZ31, b – AZ61 and c – AZ80

**Hot tensile test.** The view of the samples after tension is shown in Fig. 2. Tensile test results show that, in tested range of parameters, the ultimate tensile strength is strictly dependent on the aluminium content and is the highest for alloy AZ80 (Fig. 2b). The stress decreases almost five times with increase of deformation temperature from 200 to 450°C. In case of reduction of area Z, which is the measure of plasticity, similar values were achieved for tested alloys during deformation in temperature 300, 350 and 400°C (Fig. 2b). It is visible in this range that the most beneficial susceptibility to deformation of tested alloys is  $Z = 86.3 \div 90.4\%$ . With temperature change, the value of contraction for alloys AZ61 and AZ80 decreases which proves the gradual deterioration of plasticity over 400°C. In case of alloy AZ31 the deformability is high also in temperature of 450°C. For lower temperatures the biggest plasticity drop is observed in case of alloy AZ80, particularly intensive in temperature of 200°C.

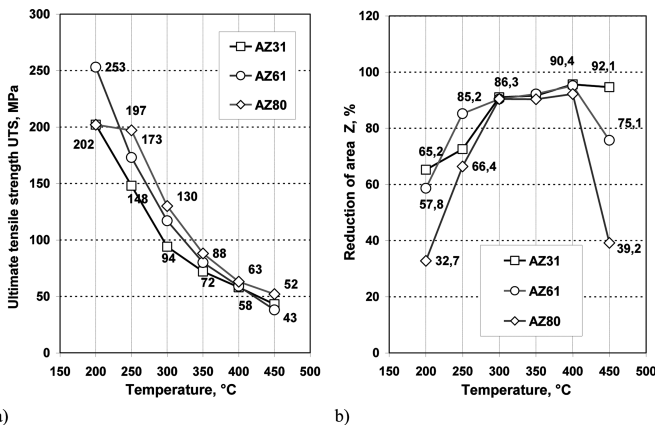


Fig. 2. Results of tensile test for investigated alloys in temperature range from 200 to 450°C, a – ultimate tensile strength (UTS), b – reduction of area (Z)

**Hot compression test.** Example flow curves which show the influence of temperature on flow stress of tested alloys AZ31, AZ61 and AZ80 are presented in Fig. 3. As it can be observed, the decrease of deformation temperature, below 300°C

changes the shape of flow curve for all tested alloys. A curve is achieved which initially has concave shape, which is connected with intensive course of twinning in microstructure.

After reaching the peak stress, together with the increase of deformation, the stress intensively drops. The smallest stress in analysed deformation temperature range was determined for alloy AZ31 (Fig. 3a) and the biggest for alloy AZ80 (Fig. 3c). Increase of strain rate also favours the achievement of characteristic course of flow stress changes during deformation within which the twinning process in microstructure takes place.

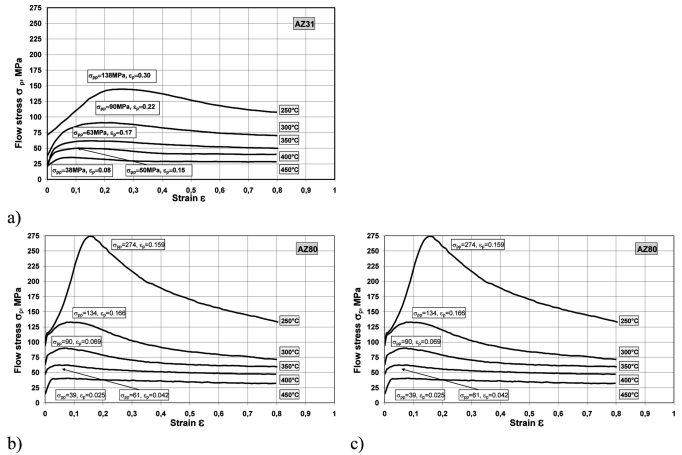


Fig. 3. Flow stress of investigated AZ31 (a), AZ61 (b) and AZ80 (c) after deformation at temperature range from 250°C to 450°C with a strain rate  $0.1s^{-1}$

The metallographic analyses (Figs. 4, 5) proved the known fact that the curves of the conventional shape (Fig. 3) arose as a result of joint influence of the dislocation hardening and the dynamic recrystallization (Fig. 4a-c), whereas the atypical curves with the concave starting phase (Fig. 3) were essentially affected by twinning. A big drop in stress after reaching the maximum is the effect of extension of surface of existing grain boundaries because of appearing twins (Fig. 5a).

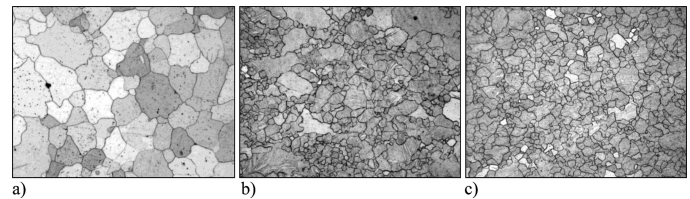


Fig. 4. The microstructure of the investigated AZ31 alloy after compression at a temperature of and 350°C – slip dominates. Strain rate of  $0.1 s^{-1}$ , strain  $\epsilon$ : a – 0.1, b – 0.4, c – 0.8

It leads to formulation of a large number of nuclei and new recrystallized grains (Fig. 5b, c), and significantly decreases the size of strain hardening.

From the values of peak stress  $\sigma_{pp}$  of particular stress-strain curves the value of the activation energy in hot forming was determined and other constants in Eqs. 2 and 6 calculated by the procedure described above. Effect of deformation heat generation was taken into account and only real and not nominal forming temperatures were considered. Similarly the mean strain rates were calculated for the relevant peak-stress values because this value can significantly differ

from the nominal value during the initial phase of compression test [12]. The calculated constants in Eqs. 2 and 6 are summarized in Table 2.

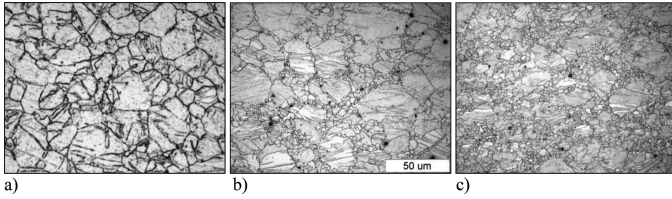


Fig. 5. The microstructure of the investigated AZ31 alloy after compression at a temperature of 250°C – twinning dominates. Strain rate of 0.1 s<sup>-1</sup>, strain ε: a – 0.1, b – 0.4, c – 0.8

TABLE 2  
Calculated constant in Eqs. 2 and 6 for investigated alloys

Alloy	AZ31 – low Z	AZ31 – high Z	AZ61	AZ80
Q [kJ/mol]	153.1	145.8	153.3	150.7
n [-]	5.67	1.50	6.47	4.04
α [MPa <sup>-1</sup> ]	0.013	0.044	0.0018	0.0080
C [s <sup>-1</sup> ]	1.04 · 10 <sup>12</sup>	3.78 · 10 <sup>9</sup>	6.37 · 10 <sup>16</sup>	6.17 · 10 <sup>11</sup>
U [-]	0.0011	0.19	0.0063	0.0066
W [-]	0.18	0.008	0.10	0.10

In the case of alloy AZ31 it was impossible to describe all experimental data by single Eqs. 2 and 6 for a wide range of experimental conditions. Previous research [12-15] disclosed that the traditional stress-strain curves of this material (as a result of dislocation hardening and dynamic recrystallization) occurred at low values of Zener-Hollomon parameter, whereas the atypical stress-strain curves with concave shape in the initial stage of deformation (essentially affected by twinning) were observed at high Z-values.

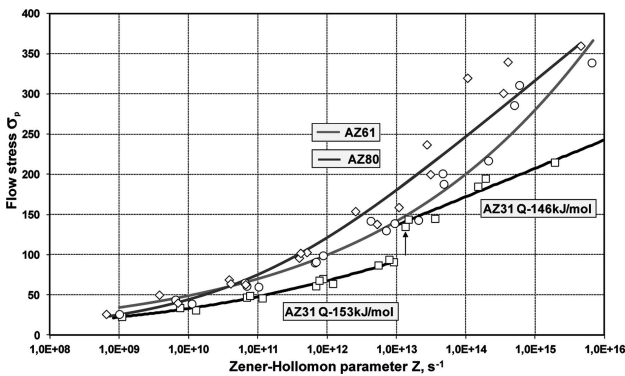


Fig. 6. Influence of Zener – Hollomon parameter (Z) on peak stress  $\sigma_{pp}$  for investigated alloy; points – experimental values, lines – calculated according to Eqs. (7)

Fig. 6 and Fig.7 shows the influence of parameter Z, appropriately on strain  $\epsilon_p$  and peak stress  $\sigma_{pp}$  from experimental data and calculated according to Eqs. 6 and 7. It is clearly visible that the dependence has exponential character. Those two deformation mechanisms were separated by the value  $Z = 9.1 \times 10^{12} \text{ s}^{-1}$ . Although the activation energy

values of alloy AZ31 are almost identical in both regions of the temperature compensated strain rate, other material constants differ substantially. Deformation behavior of alloy AZ31 at high Z-values is very specific even in comparison with other examined magnesium alloys (compare the constants in Table 2). Kinetics of the dynamic recrystallization of alloy AZ31 related to peak strain  $\epsilon_p$  is almost independent on the forming parameters for the values of  $Z > 9.1 \times 10^{12} \text{ s}^{-1}$ . Moreover, it is remarkable how slight the Q-value is of the tested materials influenced by their chemical composition. Together with the increase of parameter Z, which means decrease of temperature and increase of strain rate, the difference between flow stress rises for tested materials (Fig. 6). For alloys AZ61 and AZ80 the stress increases more intensively in comparison with alloy AZ31. The calculated strain  $\epsilon_p$  is highest for AZ31 alloy and very similar to both AZ61 and AZ80 alloy (Fig. 7).

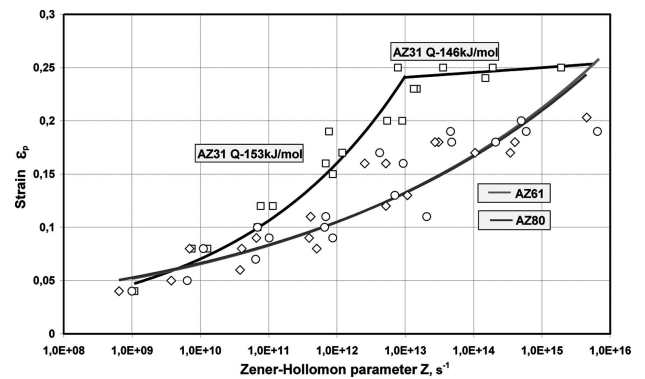


Fig. 7. Influence of Zener – Hollomon parameter (Z) on strain  $\epsilon_p$  corresponding to peak stress  $\sigma_{pp}$  for investigated alloys; points – experimental values, lines – calculated according to Eqs. (6)

Microstructures of tested AZ61 and AZ80 alloys after deformation in temperatures 250, 300, and 350 with strain rate of 0.1 s<sup>-1</sup> to deformation  $\epsilon = 0.8$  are shown in Figs 8, 9. In case of alloys AZ61 and AZ80, during deformation at temperature of 250°C small recrystallized grains are observed on grain boundaries of primary grains, but for alloy AZ61 the process is more advanced. Due to very small recrystallized grains achieved at temperature 250°C the quantitative assessment of grain size for those parameters with the use of light microscopy is practically impossible. It is clearly visible that the biggest susceptibility to recrystallization process is found in alloy AZ61 with the medium aluminium content. Microstructure is fully recrystallized after compression in temperature of 300°C similarly how in AZ31 alloy. In microstructure of AZ80 alloy primary grains are observed (Fig. 9b).

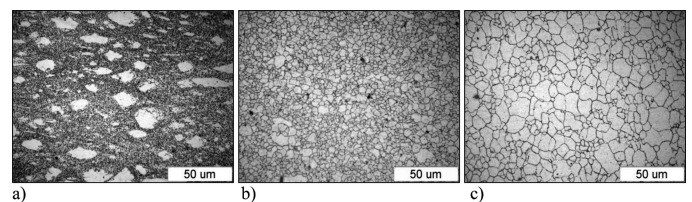


Fig. 8. Microstructure of AZ61 alloy after compression with strain rate of 0.1 to deformation  $\epsilon = 0.8$ . Deformation temperature: a – 250°C, b – 300°C, c – 350°C

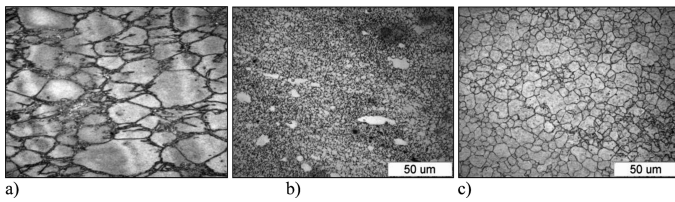


Fig. 9. Microstructure of AZ80 alloy after compression with strain rate of 0.1 to deformation  $\varepsilon = 0.8$ . Deformation temperature: a – 250°C, b – 300°C, c – 350°C

#### 4. Discussion

The paper presents analysis of magnesium alloys from AZ group with different aluminium content which beneficially influences the resistance. The fault of those alloys is relatively small deformability, particularly in lower temperatures which drops with the increase of aluminium content. Achieved data suggests that tested alloys can be formed with the methods of hot working. The most beneficial deformability described with the use of contraction  $Z$ , in tested range of changeability of deformation process parameters, can be found in alloy type AZ31 with smallest aluminium content (3%) (Fig. 2). Alloys of type AZ61 and AZ80 have comparable deformability to alloy AZ31 in temperature 300–400°C, which proves a similar value of contraction. In lower temperature the deformability decreases, particularly for alloy AZ80. Together with the increase of temperature to above 450°C, a decrease of deformability is observed, which can be connected with the fact of gradual approaching to temperature of plasticity loss (because in alloys with highest aluminium content fusible eutectics are formed).

Tests results of the influence of compression parameters on the flow stress show that it occurs with the increase of aluminium content in its structure (Fig. 3). Decrease of process temperatures leads to a stoppage, an unusual course of flow stress changes and the curve has initially concave shape. It results from gradual decrease of slip systems together with decrease of temperature and increase of participation of twinning formulation in such conditions (Fig. 5). Appearance of a new boundary decreases the dislocation mobility which causes an intensive increase of strain hardening.

Alloys are characterised by similar sensitivity to changes in deformation process temperatures, which can be read from similar values of activation energy  $Q$  (Table 2) In comparison, activation energy for self lattice diffusion of Mg is estimated at 135 kJ/mol [16]. Similar results for AZ31 alloy were obtained by authors of paper [17] when they examined the alloy AZ31 in the temperature range 250–500°C and wide range of strain rates  $10^{-4} - 10^2 \text{ s}^{-1}$ . The resulting activation energy equalled  $Q = 148 \text{ kJ/mol}$ , or  $152 \text{ kJ/mol}$ , in dependence on different deformation mechanisms. Authors of paper [5] calculated the value  $Q = 140 \text{ kJ/mol}^{-1}$  for the extruded at temperature AZ61 alloy. For alloy AZ81 the value  $Q = 180 \text{ kJ/mol}^{-1}$  was reported in paper [18].

Change of the peak flow stress ( $\sigma_{pp}$ ) in Zener-Hollomon function for tested alloys AZ61 and AZ80 can be described with the use of power function (Fig. 6) similarly to deformation  $\varepsilon_p$  (Fig. 7) for alloys AZ61 and AZ80. Alloy AZ31 behaves in a more complex way.

Difference in flow stress changes together with the increase of parameter  $Z$  for tested alloys can be explained by conducted observations of microstructure. Alloys AZ31 and are characterised by the bigger susceptibility to recrystallization process in comparison to AZ80 alloy (Figs. 4c, 5c, 8 and 9). For alloy AZ80, a smaller susceptibility to recrystallization is observed in temperature of 300°C and lower which is presented by surface taken up by recrystallized grains. In microstructure of alloy AZ80 the presence of intermetallic phase  $\gamma$  ( $\text{Mg}_{17}\text{Al}_{12}$ ). It favours a bigger dislocation hardening and faster concentration of defects which is not compensated with process of microstructure reconstruction which, as a result, leads to deformability drop, similar behaviour was reported in paper [11]. Decrease of process temperature, however, favours an achievement of fine-grained microstructure which is beneficial from the point of view of plasticity boundary.

#### 5. Conclusion

Designing the technology of plastic processing of construction elements requires a precise determination of influence of process parameters on plasticity and microstructure of alloys. It has a significant meaning when designing products made of magnesium alloys which are to be used as construction elements for aviation industry and which are supposed to replace the currently used conventional products. The advantages of magnesium are shown in many papers [1-4, 19]. Products with better set of mechanical properties can be achieved with the use of plastic processing in comparison to products achieved with the use of casting [20]. In case of alloys AZ61 and AZ80, together with the increase of aluminium content the temperature range when plastic processing can be performed gets limited, referring both of the beginning and the end of process. It requires, though, a bigger regime in conduction of the process not to lead to cracking of the product or alloy AZ31 the temperature range is biggest. The case of the examined magnesium alloys are specific because its deformation behaviour is influenced by twinning. The deformation mechanism playing an important role at high values of the temperature compensated strain rate – Zener-Hollomon parameter. Conducted microstructure tests show that for tested alloys in conditions of deformation a fine-grained microstructure can be achieved. Achieved results will provide data for computer simulation of the process of hot forging which is essential for preparation of forging technology of precise construction elements for aviation industry.

#### Acknowledgements

Financial support of Structural Funds in the Operational Programme – Innovative Economy (IE OP) financed from the European Regional Development Fund - Project "Modern material technologies in aerospace industry", No POIG.0101.02-00-015/08 is gratefully acknowledged. This paper was created also in the project No. CZ.1.05/2.1.00/01.0040 "Regional Materials Science and Technology Centre" within the frame of the operation programme "Research and Development for Innovations" financed by the Structural Funds and from the state budget of the Czech Republic.

## REFERENCES

- [1] Z. Yang, J.P. Li, J.X. Zhang, G.W. Lorimer, *Acta Metall. Sinica* **5**, 313-328 (2008).
- [2] H. Watari, R. Paisarn, T. Haga, K. Noda, *Journal of Achievements in Materials and Manufacturing Engineering* **20**, 447-450 (2007).
- [3] F. Pan, Y. Mingbo, M. Yanlong, G. Cole, *Mat. Sc. For. Vols.* **546-549**, 37-48 (2007).
- [4] T. Al-Samman, *Acta Materialia* **57**, 2229-2242 (2009).
- [5] H. Wu, J. Yang, J. Liao, F. Zhu, *Materials Science and Engineering A* **535**, 68-75 (2012).
- [6] C. Zener, J.H. Hollomon, *J. Appl. Phys.* **15** (1), 22-32 (1944).
- [7] C.M. Sellars, W.J. McG. Tegart, *Int. Metall. Rev.* **17** (1), 1-24 (1972).
- [8] I. Schindler, J. Bořuta, *Utilization Potentialities of the Torsion Plastometer*, Silesian Technical University 1998.
- [9] J. Kliber, I. Schindler, *Steel research international* **60**, 82-91 (1989).
- [10] D. Kuc, E. Hadasik, I. Bednarczyk, *Solid State Phenomena* **191**, 101-106 (2012).
- [11] P. Changizian, A. Zarei-Hanzaki, H.R. Abedi, *Materials Science and Engineering A* **558**, 44-51 (2012).
- [12] I. Schindler, P. Kawulok, R. Kawulok, E. Hadasik, D. Kuc, *High Temperature Materials and Processes* **22**, 3, 890-897 (2012).
- [13] I. Schindler, P. Kawulok, E. Hadasik, D. Kuc, *Journal of Materials Engineering and Performance*, in press.
- [14] E. Hadasik, D. Kuc, *Acta Metall. Slovaca* **16** (4), 261-267 (2010).
- [15] M. Legerski, J. Plura, I. Schindler, S. Ruzs, P. Kawulok, H. Kulveitová, E. Hadasik, D. Kuc, G. Niewielski, *High Temp. Mater. Processes* **30** (1-2), 63-69 (2011).
- [16] H. Kim, W. Kim, *Mater. Sci. Eng. A* **385**, 300-30 (2004).
- [17] B.H. Lee, K.S. Shin, C.S. Lee, *High Temperature Deformation Behavior of AZ31 Mg Alloy*, *Mater. Sci. Forum* **475-479**, 2927-2930 (2005).
- [18] P. Changizian, A. Zarei-Hanzaki, A. Roostaei, *Materials and Design* **39**, 384-389 (2012).
- [19] J. Tomczak, Z. Pater, T. Bulzak, *Archives of Metallurgy and Materials* **58**, 1, 1211-1218 (2012).
- [20] B. Płonka, J. Kut, P. Korczak, M. Lech-Gregga, M. Rajda, *Archives of Metallurgy and Materials* **57**, 4, 619-626 (2012).